PERGAMON

International Journal of Heat and Mass Transfer 44 (2001) 17–28

International Journal of HEAT and MASS TRANSFER

www.elsevier.com/locate/ijhmt

Nucleate pool boiling on structured enhanced tubes having pores with connecting gaps

Nae-Hyun Kim*, Kuk-Kwang Choi

Department of Mechanical Engineering, University of Inchon, #177 Dohwa-Dong, Nam-Gu, Inchon 402-749, South Korea

Received 30 September 1999; received in revised form 2 March 2000

Abstract

In this study, pool boiling test results are provided for the structured enhanced tubes having pores with connecting gaps. The surface geometry of the present tube is similar to that of Turbo-B. Three tubes with different pore size (0.20, 0.23 and 0.27 mm) were manufactured and tested using R-11, R-123 and R-134a. The pore size which yields the maximum heat transfer coefficient varied depending on the refrigerant. For R-134a, the maximum heat transfer coefficient was obtained for the tube having 0.27 mm pore size. For R-11 and R-123, the optimum pore size was 0.23 mm. One novel feature of the present tubes is that their boiling curves do not show a 'cross-over' characteristic, which existing pored tubes do. The connecting gaps of the present tubes are believed to serve an additional route for the liquid supply and delay the dry-out of the tunnel. The present tubes yield the heat transfer coefficients approximately equal to those of the existing pored enhanced tubes. At the heat flux 40 kW/m^2 and saturation temperature 4.4°C, the heat transfer coefficients of the present tubes are 6.5 times larger for R-11, 6.0 times larger for R-123 and 5.0 times larger for R-134a than that of the smooth tube.

Keywords: Structured enhanced tube; Pore; Gap; Nucleate pool boiling; R-11; R-123; R-134a

1. Introduction

Structured enhanced boiling tubes, which are made by reforming the base surface to make fins of a standard or special configuration, are widely used in refrigeration and process industries. Webb [1] and Thome [2] have surveyed the techniques used to develop the enhanced boiling surfaces. Structured surfaces may be categorized into three groups; those having surface pores such as Hitachi Thermoexel-E, those having narrow gaps such as Wieland GEWA-T or Trane bent-fin, and those having pores with connecting gaps such as Wolverine Turbo-B. Characteristic dimensions of the surfaces are illustrated in Fig. 1.

A systematic study on the boiling performance of tubes having surface pores has been performed by Chien and Webb [3,4]. They investigated the effect of pore diameter, pore pitch and tunnel shape using R-11 and R-123. They found that the boiling characteristics are strongly dependent on those parameters. There existed a preferred pore diameter and pore pitch for a specific heat flux range. At a low heat flux, tubes having smaller 'total open area' (defined as sum of pore areas) yielded higher heat transfer coefficients, while, at a high heat flux, tubes

* Corresponding author. Tel.: +82-32-770-8420; fax: +82-32-770-8410.

E-mail address: knh0001@lion.inchon.ac.kr (N.-H. Kim).

0017-9310/01/$ - see front matter
PII: S0017-9310(00)00096-X

Nomenclature

d_p	pore diameter (m)	P_{p1}	circumferential pore pitch (m)
h	heat transfer coefficient (W/m^2 K)	P_{p2}	neighboring pore pitch (m)
H_t	tunnel height (m)	P_{red}	reduced pressure, dimensionless ($= P/P_c$)
P	pressure (N/m^2)	P_w	wetted perimeter (m)
P_c	critical pressure (N/m^2)	q''	heat flux (W/m^2)
P_f	fin pitch (m)	T_{sat}	saturation temperature (K)
P_p	pore pitch (m)	T_w	tube wall temperature (K)

having larger total open area yielded higher heat transfer coefficients. The 'cross-over' characteristic of the boiling curves is illustrated in Fig. 2. If the total open area is too large at a low heat flux, the tunnel is likely to be flooded by the liquid, and the heat transfer coefficient is decreased. If the open area is too small at a high heat flux, the tunnel will dry out due to the insufficient liquid supply. Similar trend was reported by Nakayama et al. [5,6] for the Themoexel-E type pored surface. Their boiling curves for R-11, water and nitrogen clearly show the 'cross-over' characteristic. The flow visualization studies on these surfaces by Chien and Webb [7,8] and Nakayama et al. [5] support the trend. The dry-out of the tunnel at a high heat flux and the flooding of the tunnel at a low heat flux were observed.

The pool boiling data of tubes having narrow gaps, however, do not show the cross-over characteristic. For example, the R-113 and water data on GEWA-T tube by Ayub and Bergles [9] show that the tube with optimum gap width outperforms the other tubes for the entire heat flux range. For these tubes, the tunnel is not likely to dry out even at a high heat flux because the liquid is continuously supplied through the gaps. The heat transfer coefficients of these tubes, however, are lower than the pored tubes as reported by Pais and Webb [10] and Thome [2]. For these tubes, some portion of the tunnel may always be flooded by the liquid because of the unconstrained liquid supply through the gaps.

Tubes having pores and gaps may exploit the advantages of both the pored tubes and the gapped ones. They may provide high heat transfer coefficients close to those of the pored tubes, while not yielding the 'cross-over' characteristic. The Wolverine Turbo-B has pores with connecting gaps. The heat transfer coeffi-

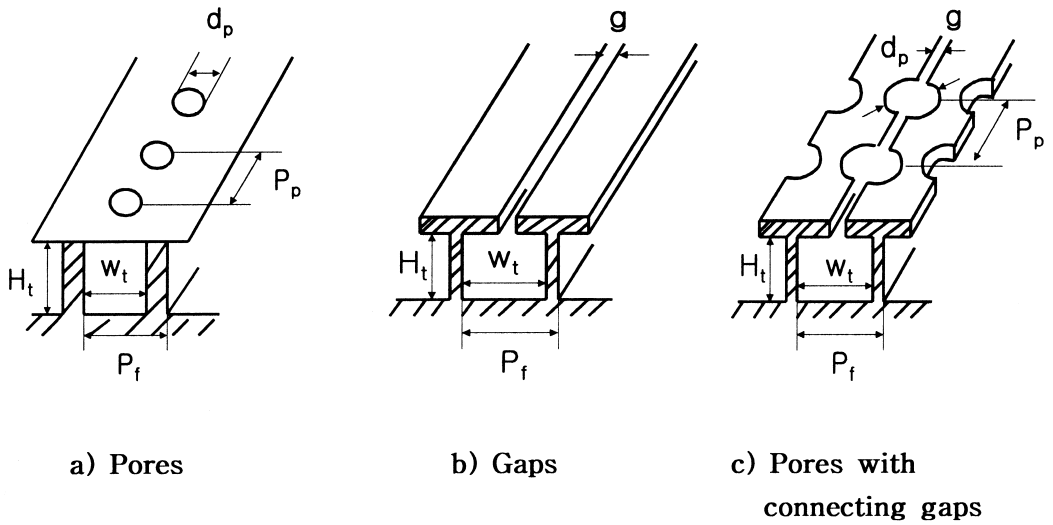

Fig. 1. Characteristic dimensions of structured enhanced tubes.

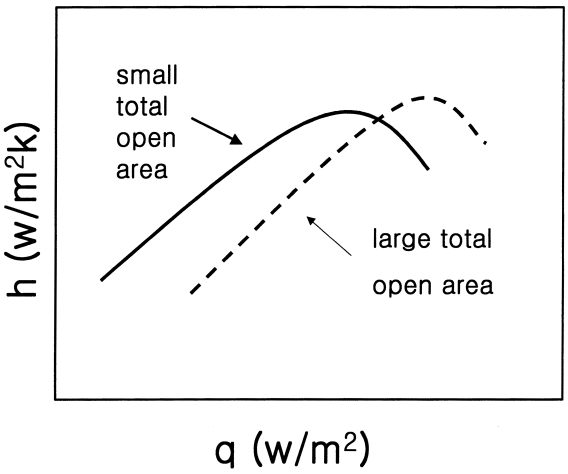

Fig. 2. 'Cross-over' characteristics of pored enhanced tubes as reported by Chien and Webb [3].

cients of Turbo-B is close to those of pored tubes such as Thermoexel-E as reported by Thome [2]. However, the effect of pore diameter of Turbo-B type tubes has not been investigated. In this study, the effect of pore size on the pool boiling characteristics of Turbo-B type enhanced tubes were investigated. The refrigerants tested include R-11, R-123 and R-134a.

2. Sample tubes

New enhanced tubes were made by a metal-forming process and the enlarged photos of the tunnels and surfaces are shown in Fig. 3. These tubes were made from low integral fin tubes having 1654 fins per meter with 1.3 mm fin height, cutting small notches (0.9 mm depth) on the fins, and then flattening the fins by a rolling process. The resultant tube had triangular pores with connecting gaps and gourd-shaped tunnels. Three tubes with different pore size (and corresponding gap width) were made. The pore size was varied by changing the pressure on the rollers. The geometric dimensions of the surfaces are listed in Table 1. The pore size in the table is represented by the diameter of a circle inscribed in a triangle. The geometric dimensions were measured from enlarged photos taken at 20 different locations. The pore size and the gap width were fairly uniform, and those listed in Table 1 are the averaged values. One notable thing of the present tube is that two pores exist per pore pitch.

3. Experimental apparatus and procedures

The test apparatus is shown in Fig. 4. The pool boiling test cell consists of a 150 mm inner diameter and 350 mm long copper tube and two flanges. The test tube was mounted on the copper flange at one end of the test cell, and the sight glass was installed on the other end of the test cell. The vapor generated during the test was condensed in the external condenser. The brine from the constant temperature bath circulated in the tube-side of the condenser. Tests were performed at two saturation temperatures (4.4°C and 26.7°C). The 4.4°C was chosen because commercial refrigeration chillers operate at the temperature and the 26.7°C was chosen because it is the normal room temperature. The apparatus had a charging line and evacuating line connected to a positive displacement vacuum pump.

The detailed sketch of the test tube is shown in Fig. 5. The enhanced tubes were specially made from thick-walled copper tubes of 18.8 mm outer diameter and 13.5 mm inner diameter. The length was 170 mm. An electric cartridge heater of 13.45 mm diameter and 180 mm long was inserted into the test tube. Its electric power was controlled by an auto-transformer. The heater was specially manufactured to contain 170 mm long heated section (same length as that of the test tube) and two 5 mm long unheated end sections. To minimize the heat loss, the unheated sections were covered with a Teflon cap and a Teflon ring as illustrated in Fig. 5. Before insertion, the heater was coated with a thermal epoxy to enhance the thermal contact with the tube.

Four thermocouple holes of 1.0 mm diameter were drilled to the center of the tube. Copper–constantan

Table 1
Geometric dimensions of the sample tubes

No.	d_p (mm)	g (mm)	P_{p1} (mm)	P_{p2} (mm)	P_f (mm)	H_t (mm)	W_t (mm)
1	0.20	0.04	0.71	0.374	0.605	0.54	0.25
2	0.23	0.07	0.71	0.384	0.605	0.54	0.25
3	0.27	0.10	0.71	0.400	0.605	0.54	0.25

thermocouples of 0.3 mm diameter per wire were inserted into the holes to measure the tube wall temperature. Before insertion, the thermocouples were coated with a thermal epoxy [Chromalox HTRC] to provide good thermal contact with the tube wall. The thermal conductivity of the epoxy is close to that of aluminum. The vapor temperature was measured at two locations on the upper part of the test cell, and the liquid temperature was measured at 20 mm above the test tube and at 20 mm below the test tube. During the test, the four temperatures agreed within 0.2°C. The test cell pressure was measured using a pressure transducer. When the measured pressure was converted to the corresponding saturation temperature, they agreed within 0.3°C.

Before each test, the test tube was thoroughly cleaned with acetone. Then, the tube surface was conditioned employing the surface aging technique "B" of Bergles and Chyu [11]. The method involved degassing the test tube and the pool at the maximum heat flux (approximately 50 kW/m^2) for 1 h. The pool was maintained close to the saturation temperature using the constant temperature bath (for 4.4°C saturation temperature) or the auxiliary heater (for 26.7°C saturation temperature). The data were taken decreasing the heat flux. Readings were taken 5–10 min after each power change, at which time a steady-state condition was attained. Before reading the data, the auxiliary heater was shut off to minimize the convective effects from the heater. Throughout the test, the liquid level was maintained at 5 cm above the test tube.

The heat transfer coefficient (h) is determined by the heat flux (q'') over wall superheat ($T_w - T_{sat}$). Calculations of q'' and h are based on the envelope area, defined by the heated length (170 mm) multiplied by the tube outside perimeter. The input power to the

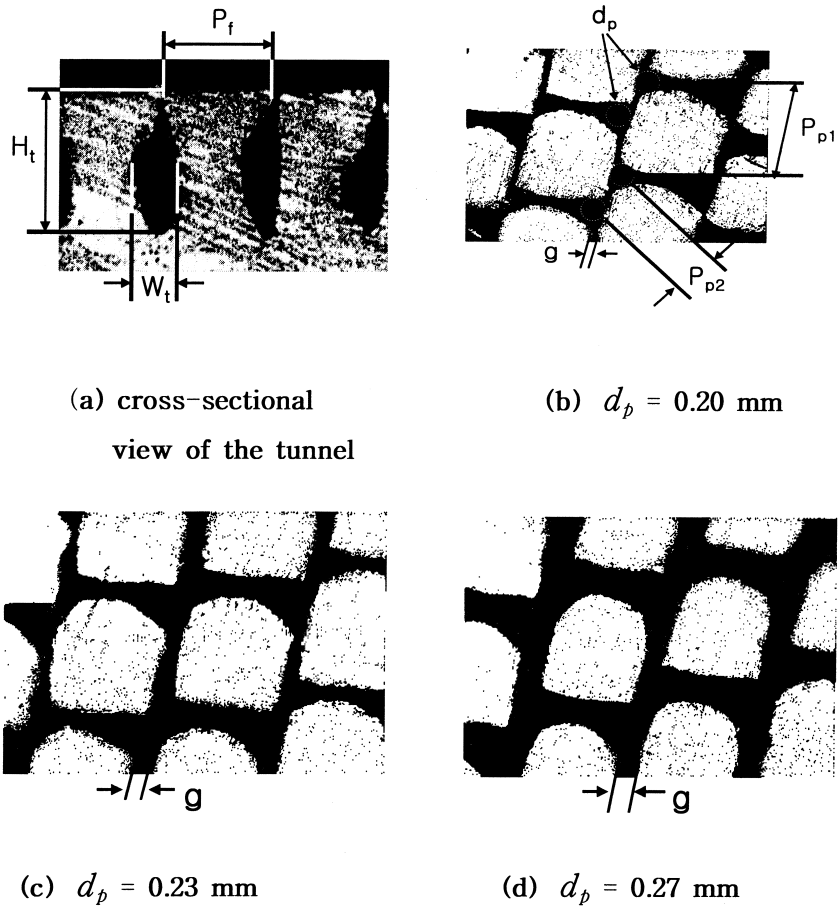

(a) cross-sectional view of the tunnel

(b) d_p = 0.20 mm

(c) d_p = 0.23 mm

(d) d_p = 0.27 mm

Fig. 3. Enlarged photos showing the present enhanced geometry: (a) cross-sectional view of the tunnel, (b) tube with $d_p = 0.20$ mm, (c) tube with $d_p = 0.23$ mm, (d) tube with $d_p = 0.27$ mm.

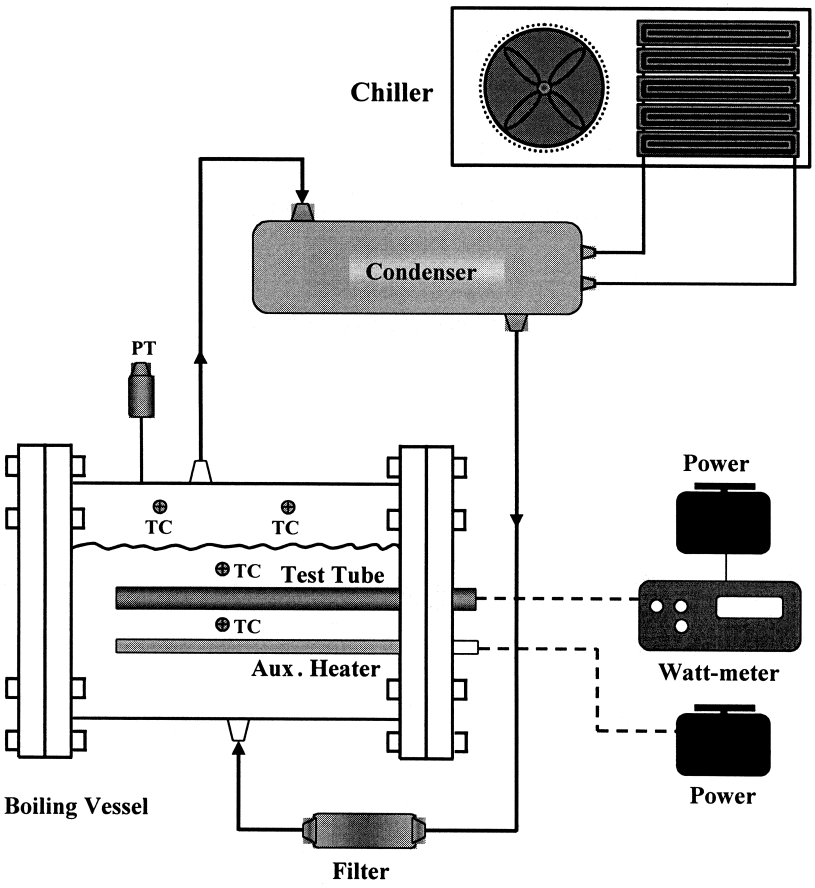

Fig. 4. Schematic drawing of the experimental apparatus.

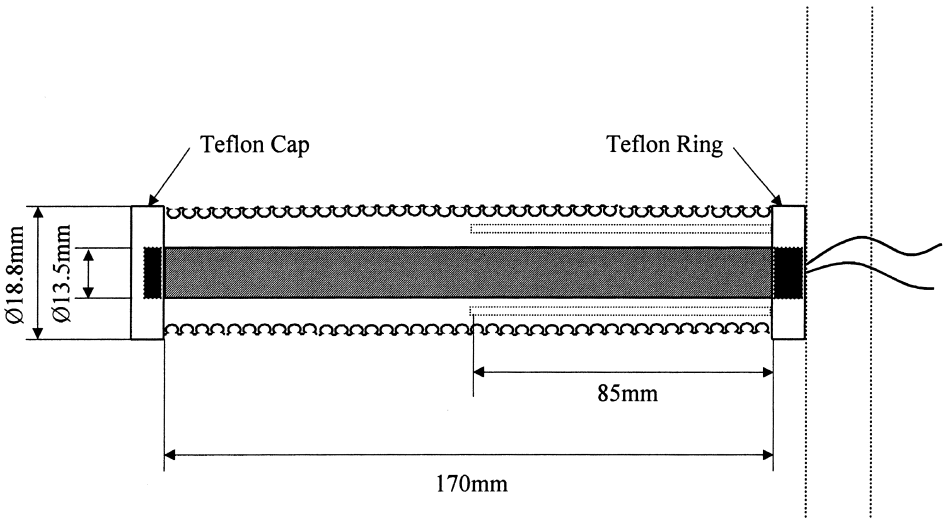

Fig. 5. Detailed sketch of the test tube.

heater was measured by a precision watt-meter [Chitai 2402A] and the thermocouples were connected to the data logger [Fluke 2645A]. The pressure transducer was also connected to the data logger. The thermocouples and the transducer were calibrated and checked for repeatability. The calculated accuracy of the temperature measurement was $\pm 0.15^{\circ}C$. Tube wall temperature was determined by extrapolating the thermocouple temperatures to the tube wall using Fourier's law.

An error analysis was conducted following the procedure proposed by Kline and McClintock [12]. The uncertainty in the heat transfer coefficient is estimated to be $\pm 3\%$ at the maximum heat flux (50 kW/m^2) and $\pm 7\%$ at a low heat flux (10 kW/m^2). The heat flux profile in axial direction may not be uniform because of the heat loss at each ends of the heater. A series of tests were conducted changing the thermocouple location in axial direction. The corresponding heat transfer coefficients agreed each other within $\pm 3\%$. All the tests were conducted with thermocouples located at the center of the tube.

4. Results and discussion

4.1. Smooth tube

Prior to the tests on enhanced tubes, tests were conducted on a smooth tube. The surface of the tube was emery ground, and the surface profile was measured using a profilometer [Kosaka Lab. SE 3300]. The arithmetic mean roughness height was 0.29 μm. After being ground, the tube was seasoned in a room about a week until a stable oxide film was formed on the surface. This was necessary because the boiling heat transfer coefficient of the just-ground tube was significantly higher than that of the seasoned tube. Several tests conducted for the seasoned tube revealed that the heat transfer coefficients were repeatable.

The boiling heat transfer coefficients of the smooth tube taken at 4.4°C saturation temperature are shown in Fig. 6. The heat transfer coefficients of R-11 and R-123 are approximately equal while those of R-134a are considerably higher. It is generally accepted that higher the reduced pressure is, higher the heat transfer coefficient becomes. At 4.4°C, the reduced pressure of R-134a is approximately eight times larger than that of R-11 or R-123. The reduced pressures of R-11 and R-123 are approximately the same. The present data are compared with the Cooper [13] correlation (using $R_p = 0.29\mu m$) in Fig. 7. Fig. 7 shows that most of the data are predicted within $\pm 10\%$. The Cooper correlation is known to predict the pool boiling data of refrigerants reasonably well.

4.2. Enhanced tubes

Visual observation on the boiling of the present enhanced tubes revealed that bubbles were generated mainly from the pores (not the gaps). As the heat flux increased, the number of active pores also increased. Similar trend was also reported by Chien and Webb [7] for the pored tubes. The experimental heat transfer coefficients of the present enhanced tubes are shown in Figs. 8–10. Fig. 8 shows the heat transfer coefficients for R-11 at two different saturation temperatures (4.4°C and 26.7°C). The figure shows that the pore size has a marked influence on the boiling performance. The maximum heat transfer coefficient is obtained for the tube with 0.23 mm pore size. Tubes with smaller ($d_p = 0.20$ mm) or larger ($d_p = 0.27$ mm) pore yielded

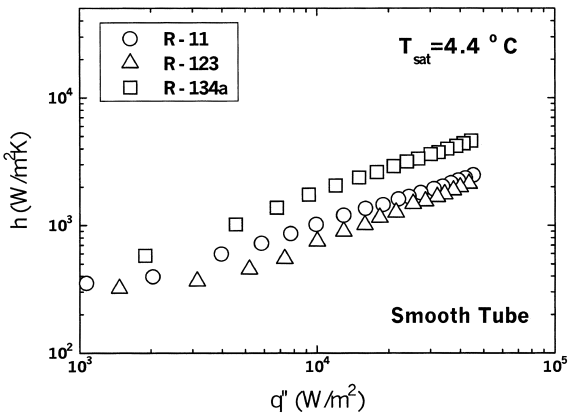

Fig. 6. Boiling heat transfer coefficients of the smooth tube at $T_{sat} = 4.4^{\circ}C$.

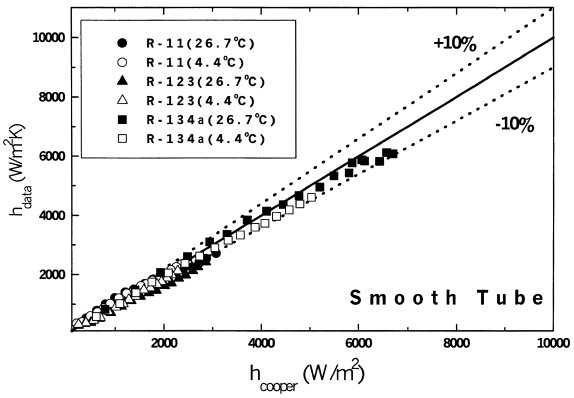

Fig. 7. Smooth tube data compared with Cooper [13] correlation.

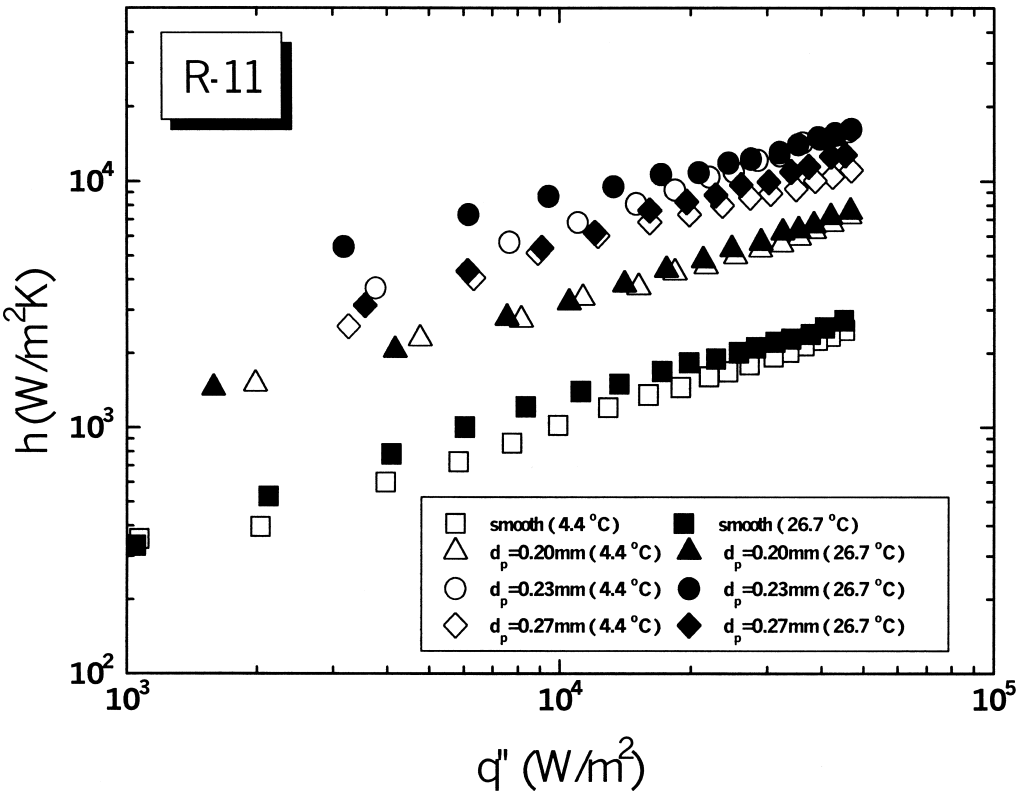

Fig. 8. A graph showing the effect of pore size for R-11.

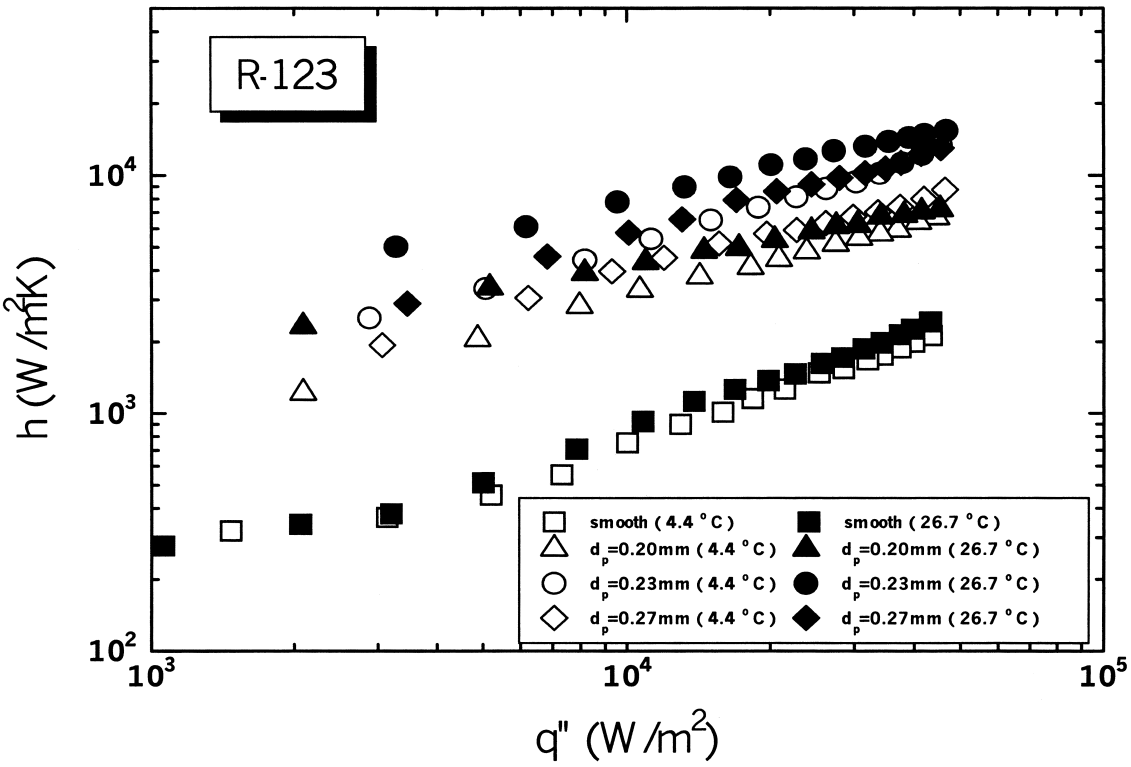

Fig. 9. A graph showing the effect of pore size for R-123.

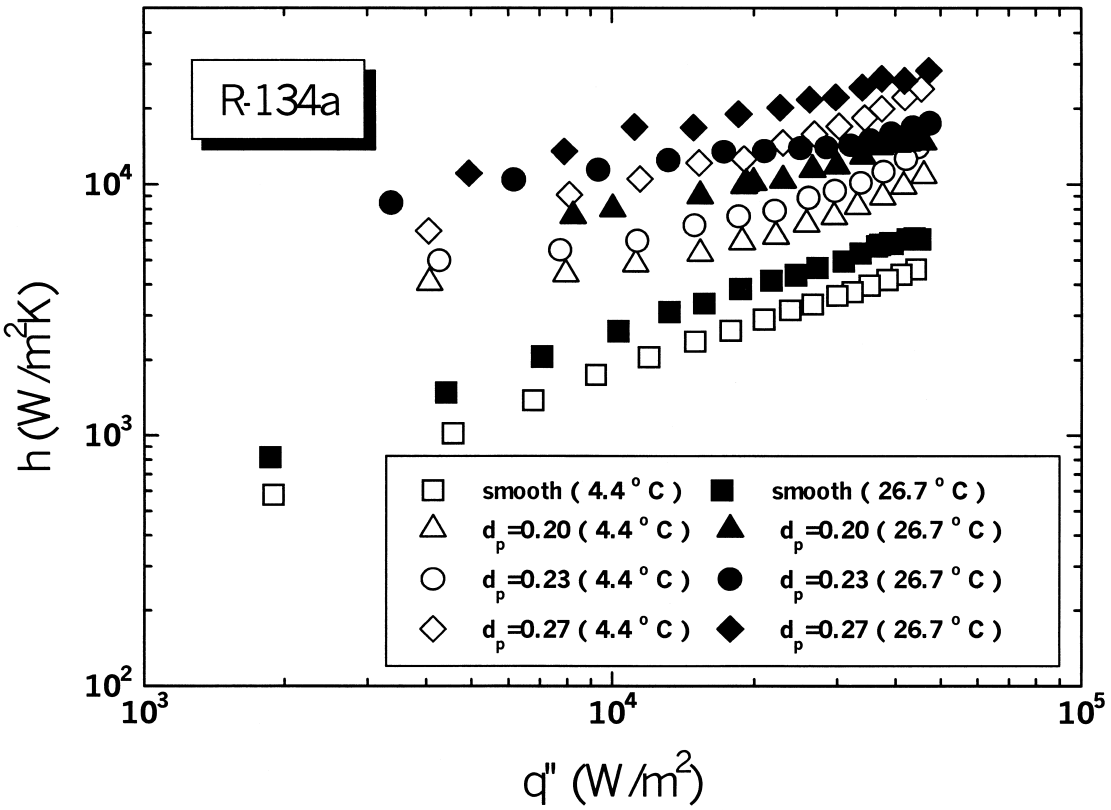

Fig. 10. A graph showing the effect of pore size for R-134a.

decreased heat transfer coefficients. As discussed by Nakayama et al. [14] and Chien and Webb [15], the maximum heat transfer is related with the just enough liquid supply into the tunnel to sustain the liquid menisci in the corners. Larger amount of liquid may flood the tunnel and smaller amount may cause dry-out of the tunnel. Fig. 8 also shows that the heat transfer coefficients at 26.7°C are slightly higher than those at 4.4°C. Higher reduced pressure at 26.7°C compared with that at 4.4°C may be responsible. At the normal operating condition of a refrigerant evaporator (4.4°C and 40 kW/m^2), the present enhanced tubes yield up to 6.5 times higher heat transfer coefficients than the smooth tube does.

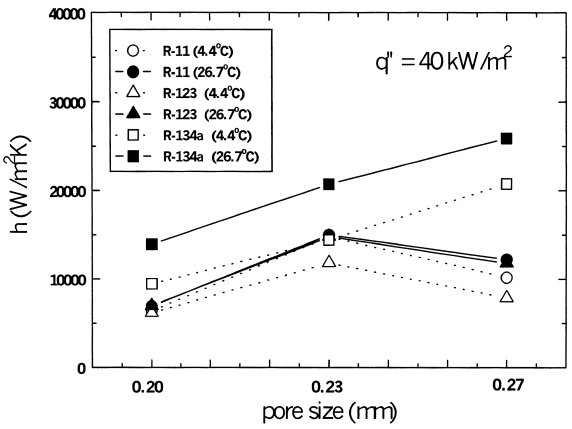

Fig. 11. A graph showing the effect of pore size for R-11, R-123 and R-134a at the heat flux 40 kW/m^2.

The heat transfer coefficients for R-123 are shown in Fig. 9. Comparison of it with Fig. 8 reveals that the heat transfer coefficients are approximately equal for both refrigerants. The maximum heat transfer coefficient is also obtained at the same pore size ($d_p = 0.23$ mm). The thermophysical properties of R-123 are similar to those of R-11, and the thermal performance for the two refrigerants is expected to be approximately equal [3,4,10]. Fig. 9 shows that the heat transfer coefficients of the present tubes are up to six times higher than that of the smooth tube at 4.4°C and 40 kW/m^2.

Fig. 10 shows the heat transfer coefficients for R-134a. Different from R-11 or R-123, the maximum heat transfer coefficient was obtained from the tube with the largest pore size ($d_p = 0.27$ mm). This trend is

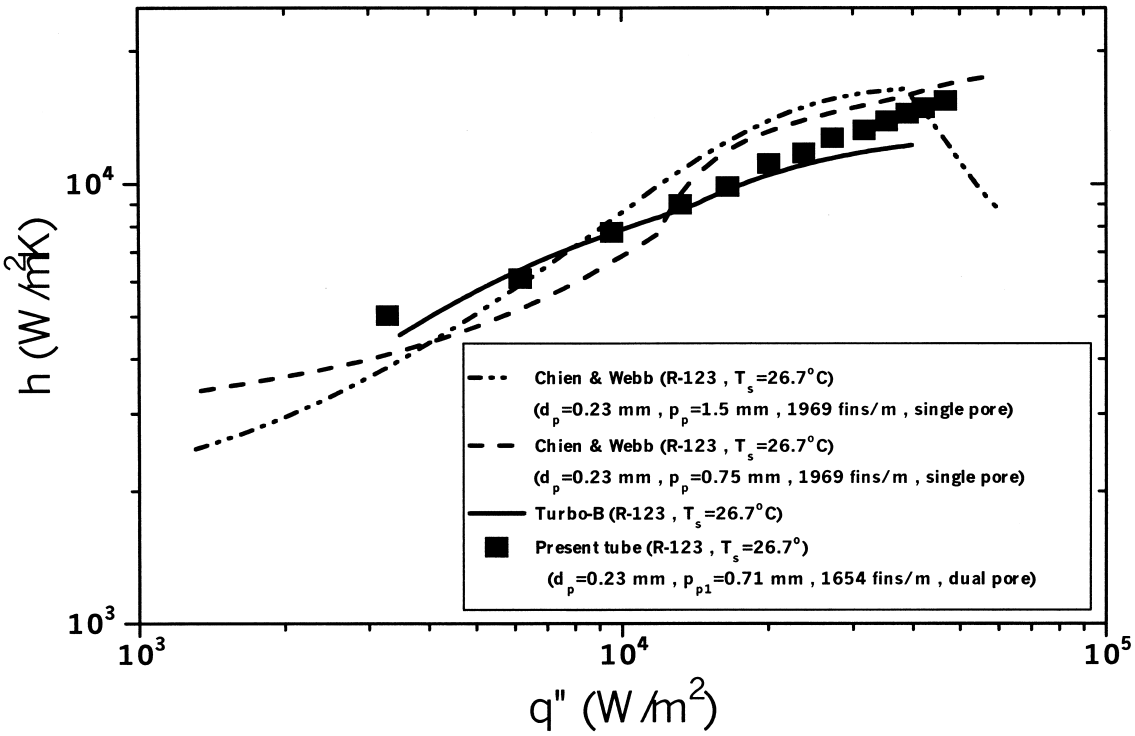

Fig. 12. The heat transfer coefficients of the present tube compared with those from other sources.

more clearly seen in Fig. 11. In Fig. 11, the heat transfer coefficients are shown as a function of pore size (at the heat flux of 40 kW/m^2). The pore size, where the maximum heat transfer coefficient is obtained, is larger for R-134a ($d_p = 0.27$ mm) when compared with that for R-11 or R-134a ($d_p = 0.23$ mm). The R-134a has a much higher (eight times at 4.4°C) reduced pressure than R-11 or R-123, and yields higher heat transfer coefficients (as shown in Fig. 11). The shift of the optimum pore size may be related with the magnitude of the reduced pressure. Nakayama et al.'s [5] investigation supports this observation. The optimum size for nitrogen ($d_p = 0.12$ mm) was larger than that of R-11 ($d_p = 0.10$ mm) for the tests conducted at atmospheric pressure. At atmospheric pressure, the reduced pressure of nitrogen is 0.030 and that of R-11 is 0.023. The optimum pore size may be obtained from the comprehensive models such as Nakayama et al. [14] or Chien and Webb [15]. The applicability of these models to the present enhanced tube is elaborated later. Fig. 10 shows that the heat transfer coefficients of the present tubes are up to five times larger than that of the smooth tube at 4.4°C and 40 kW/m^2.

In Fig. 12, the heat transfer coefficients of the present enhanced tube are compared with those of other pored enhanced tubes (Chien and Webb [3], and Pais and Webb [10]) for R-123 at 26.7°C saturation temperature. All the data correspond to the pore size which provides the maximum heat transfer coefficients. Chien and Webb's data are from the tubes having different circumferential pore pitches; one ($P_p = 0.75$ mm) close to the circumferential pore pitch of the present tube ($P_{p1} = 0.71$ mm), the other ($P_p = 1.5$ mm) almost twice larger than the present one. The Chien and Webb's tube has 1969 fins per meter, circular pores and one pore per circumferential pore pitch. The present tube has 1654 fins per meter, triangular pores and dual pores per circumferential pore pitch. The fin density of Chien and Webb's tube is approximately 20% larger than that of the present tube. The effect of fin density of the pored tubes has been investigated by Chien [16], who concluded that the fin density has only a secondary effect, at least within his test range (from 1575 fins per meter to 1969 fins per meter).

Fig. 12 shows that the heat transfer coefficients of the present tube are approximately the same as those of Chien and Webb's tube having 0.75 mm pore pitch. The circumferential pore pitches of the two tubes are close each other. The total open area of the present tube (1654 fins per meter, 0.23 mm pore size, dual pore per 0.71 mm pore pitch), however, is 1.8 times larger than that of Chien and Webb's tube (1969 fins

per meter, 0.23 mm pore size, single pore per 0.75 mm pore pitch). Chien and Webb's tube having 1.5 mm pore pitch yields slightly higher heat transfer coefficients up to $q'' = 40$ kW/m^2, and then the heat transfer coefficients drop off. The present tube do not show the drop-off characteristic (at least up to $q'' = 50$ kW/m^2). It is believed that the connecting gaps of the present tube act as an additional route for liquid supply, and delay the dryout in the tunnel. The total open area of Chien and Webb's $P_p = 1.5$ mm tube is approximately the same as that of the present tube. Also shown in the figure are the heat transfer coefficients of Turbo-B [10]. The heat transfer coefficients of the present tube are approximately the same as those of Turbo-B.

Literature shows several models and correlations applicable to enhanced boiling surfaces. Survey on this issue is provided in the monographs by Webb [1] and Thome [2]. The first analytic model accounting for the dynamic nature of bubble generation has been developed by Nakayama et al. [14]. Their model is applicable to Thermoexel-E type surfaces. Nakayama et al. assumed that the total heat flux is the sum of the tunnel heat flux due to thin film evaporation and the sensible heat flux due to external convection. Based on the sequence of events during a cycle of bubble growth and departure, they derived the predictive equations. Their equations, however, had eight empirical constants. In addition, the constants differed for different fluid or pore size. Nakayama et al. presented the constants for R-11 for the two pore sizes ($d_p = 0.04$ mm and 0.10 mm) they tested. The pores of the present tubes are larger than those of Nakayama et al.'s tubes. Recently, Chien and Webb [15] developed a comprehensive model applicable to pored tubes. They improved Nakayama et al.'s model accounting for the temporal evaporation rate inside tunnels, which Nakayama et al. treated as empirical constants. Their model requires only two empirical constants. One important parameter in Chien and Webb's model is the number of liquid menisci in the tunnel, where the thin liquid film evaporates. For well-defined tunnel shapes such as U-shape or rectangular shape, the number of

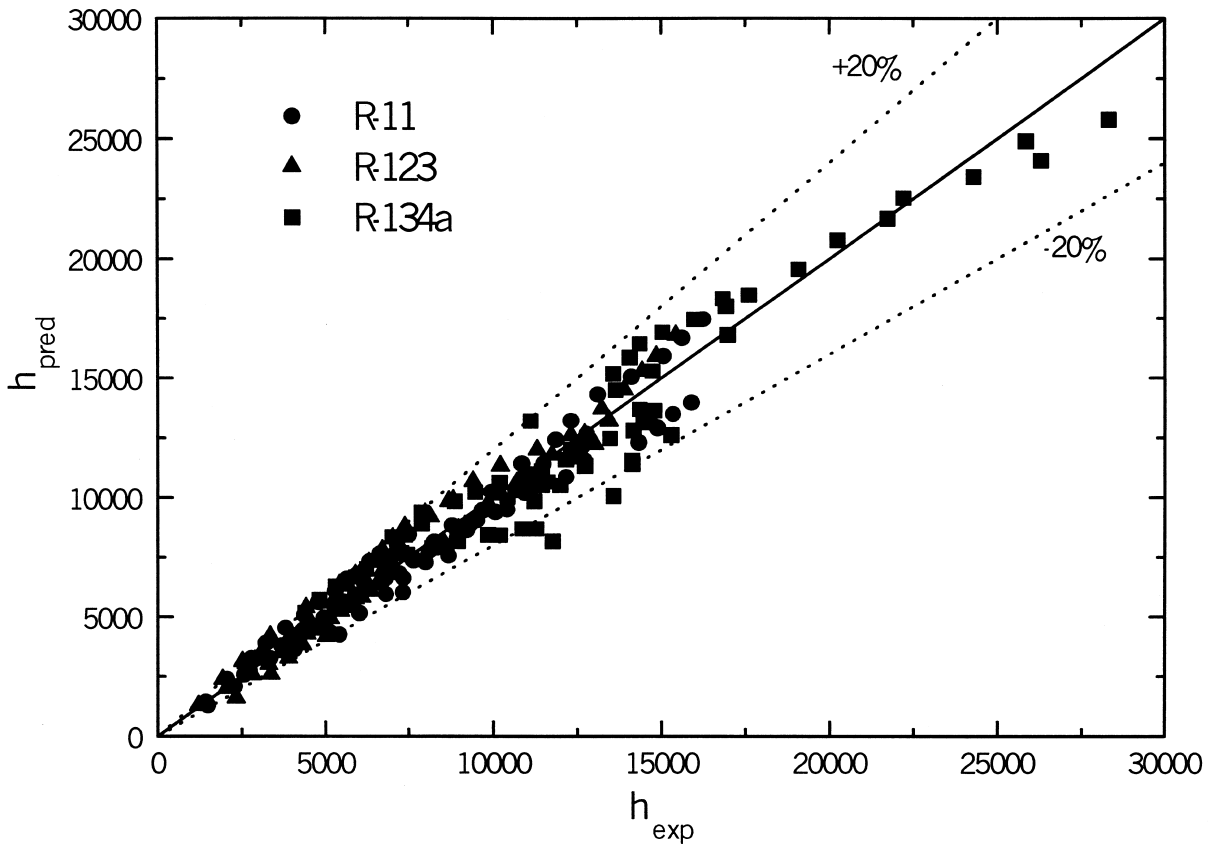

Fig. 13. The present data compared with the correlation (Eqs. (1) and (2)).

liquid menisci may be clearly determined (two for the U-shaped tunnel and four for the rectangular shaped tunnel). Most commercial tubes including the present ones, however, have tunnels of an irregular shape as shown in Fig. 2. The irregular tunnel shape provides a crucial uncertainty in applying the model to the present tube.

Because the existing models are not directly applicable to the performance prediction of the present tubes, an effort was made to develop a correlation. The correlation has parameters proposed by Cooper [13] for the plain tube, and an additional parameter (pore diameter) to include the effect of pore size. An attempt had been made to develop a single correlation using all the present data (R-11, R-123 and R-134a). The effort was not so successful, mainly because the trend of the pore size was different for different refrigerants, as shown in Fig. 11. For R-11 and R-123, the heat transfer coefficients show an optimum value at $d_p = 0.23$ mm, while they continuously increase as the pore size increases for R-134a. Thus, a separate correlation was developed for R-134a. The correlations are given by

R-11 and R-123:

$$h = 112.2q^{0.523}P_{red}^{0.254}\left(-1.13 - 9.76\times10^{4}d_p + 9.40\times10^{8}d_p^2 - 2.03\times10^{12}d_p^3\right) \quad (1)$$

R-134a:

$$h = 1.0\times10^{11}q^{0.297}P_{red}^{0.632}d_p^{2.1} \quad (2)$$

Fig. 13 shows that the correlation predicts all the data within $\pm 20\%$.

5. Conclusions

In this study, pool boiling tests were conducted for the structured enhanced tubes having pores with connecting gaps. Listed below are the major findings.

1. The pore size where the maximum heat transfer coefficient is obtained is larger for R-134a ($d_p = 0.27$ mm) compared with that for R-11 or R-134a ($d_p = 0.23$ mm). The higher reduced pressure of R-134a may be related with this shift.
2. The boiling curves of the present tubes do not show a 'cross-over' characteristic, which existing pored tubes do. The connecting gaps of the present tube are believed to act as an additional route for the liquid supply and delay the dry-out of the tunnel.
3. The present tubes yield the heat transfer coefficients approximately equal to those of the existing pored enhanced tubes. At the heat flux 40 kW/m^2 and saturation temperature 4.4°C, the heat transfer coefficients of the present tubes are 6.5 times larger for R-11, 6.0 times larger for R-123 and 5.0 times larger for R-134a than that of the smooth tube.

Acknowledgements

The fund for present study has been provided by the R&D Management Center for Energy and Resources of Korea, which is appreciated.

References

[1] R.L. Webb, Principles of Enhanced Heat Transfer, Wiley/Interscience, New York, 1999 (Chapter 11).
[2] J.R. Thome, Enhanced Boiling Heat Transfer, Hemisphere, New York, 1990.
[3] L.-H. Chien, R.L. Webb, A parametric study of nucleate boiling on structured surfaces, Part I: effect of tunnel dimensions, Journal of Heat Transfer 120 (1998) 1042–1048.
[4] L.-H. Chien, R.L. Webb, A parametric study of nucleate boiling on structured surfaces, Part II: effect of pore diameter and pore pitch, Journal of Heat Transfer 120 (1998) 1049–1054.
[5] W. Nakayama, T. Daikoku, H. Kuwahara, T. Nakajima, Dynamic model of enhanced boiling heat transfer on porous surfaces, Part I: experimental investigation, Journal of Heat Transfer 102 (1980) 445–450.
[6] W. Nakayama, T. Daikoku, T. Nakajima, Effect of pore diameters and system pressure on saturated pool nucleate boiling heat transfer from porous surfaces, Journal of Heat Transfer 104 (1982) 286–291.
[7] L.-H. Chien, R.L. Webb, Measurement of bubble dynamics on an enhanced boiling surface, Experimental Thermal Fluid Science, 16 (1998) 177–186.
[8] L.-H. Chien, R.L. Webb, Visualization of pool boiling on enhanced surfaces, Experimental Thermal Fluid Science 16 (1998) 332–341.
[9] Z.H. Ayub, A.E. Bergles, Pool boiling from GEWA surfaces in water and R-113, Warme- und-Stoffubertragung 21 (1987) 209–219.
[10] R.L. Webb, C. Pais, Nucleate pool boiling data for five refrigerants on plain, integral-fin and enhanced tube geometries, International Journal of Heat and Mass Transfer 35 (8) (1992) 893–1904.
[11] A.E. Bergles, M.C. Chyu, Characteristics of nucleate pool boiling from porous metallic coatings, Journal of Heat Transfer 104 (1982) 279–285.
[12] S.J. Kline, F.A. McClintock, The description of uncertainties in single sample experiments, Mechanical Engineering 75 (1953) 3–9.

[13] M.G. Cooper, Correlations for nucleate boiling: formulation using reduced properties, Physico-Chemical Hydrodynamics 3 (2) (1982) 89–111.
[14] W. Nakayama, T. Daikoku, H. Kuwahara, T. Nakajima, Dynamic model of enhanced boiling heat transfer on porous surfaces, Part II: analytical modeling, Journal of Heat Transfer 102 (1980) 451–456.
[15] L.-H. Chien, R.L. Webb, A nucleate boiling model for structured enhanced surfaces, International Journal of Heat and Mass Transfer 41 (14) (1998) 2183–2195.
[16] L.-H. Chien, Mechanism and analysis of nucleate boiling on structured surfaces, PhD thesis, The Pennsylvania State University, University Park, PA, 1996.